

LU TP 98-10
December 2, 2024

Design of Sequences with Good Folding Properties in Coarse-Grained Protein Models

Anders Irbäck¹, Carsten Peterson²,
Frank Potthast^{3,4} and Erik Sandelin⁵

Complex Systems Group, Department of Theoretical Physics
University of Lund, Sölvegatan 14A, S-223 62 Lund, Sweden
<http://www.thep.lu.se/tf2/complex/>

Submitted to *Folding and Design*

Background: Designing amino acid sequences that are stable in given a target structure amounts to maximizing a conditional probability. A straightforward approach to accomplish this is a nested Monte Carlo where the conformation space is explored over and over again for different fixed sequences, which requires excessive computational demand. Several approximate attempts to remedy this situation, based on energy minimization for fixed structure or high- T expansions, have been proposed. These methods are fast but often not accurate since folding occurs at relatively low T .

Results: We develop a multisequence Monte Carlo procedure, where both sequence and conformation space are simultaneously probed with efficient prescriptions for pruning sequence space. Whenever feasible, the method is compared with exact results and with other methods for lattice and off-lattice two-letter code minimalist models with sizes ranging from $N = 16$ to 50.

Conclusions: The multisequence Monte Carlo methods shows quite some promise. The resulting performance is very good with respect to both solution quality and computational effort for all problems probed. As a by-product signatures for cooperativity in $N = 50$ two-dimensional lattice chains are obtained. This observation is in contrast to general belief.

Correspondence: Anders Irbäck
e-mail: irback@thep.lu.se

Key words: lattice models, Monte Carlo methods, off-lattice models, protein design, protein folding

¹irback@thep.lu.se

²carsten@thep.lu.se

³frank@thep.lu.se

⁴Current address: Astra Hässle AB, Preclinical R&D, Research Informatics, S-431 83 Mölndal, Sweden.

⁵erik@thep.lu.se

1 Introduction

The protein design problem amounts to finding an amino acid sequence given a target structure, which is stable in the target structure, and is able to fold fast into this structure. In a typical model the second requirement implies that stability must set in at not too low a temperature. Hence, one is led to consider the problem of finding sequences that maximize the stability of the target structure at a given temperature. In terms of a model described by an energy function $E(r, \sigma)$, where $r = \{\mathbf{r}_1, \mathbf{r}_2, \dots, \mathbf{r}_N\}$ denotes the structure coordinates and $\sigma = \{\sigma_1, \sigma_2, \dots, \sigma_N\}$ the amino acid sequence, this can be expressed as maximizing the conditional probability

$$P(r_0|\sigma) = \frac{1}{Z(\sigma)} \exp[-E(r_0, \sigma)/T], \quad (1)$$

where r_0 denotes the target structure, T the temperature and the partition function $Z(\sigma)$ is given by

$$Z(\sigma) = \sum_r \exp[-E(r, \sigma)/T]. \quad (2)$$

Maximizing $P(r_0|\sigma)$ with respect to σ represents quite some challenge, since for any move in σ , the partition function $Z(\sigma)$ needs to be evaluated; each evaluation of $P(r_0|\sigma)$ effectively amounts to a folding calculation for fixed sequence σ .

Different ways of handling this sequence optimization problem have been proposed and partly explored in the context of coarse-grained (or minimalist) protein models, where amino acid residues represent the entities. The proposed methods fall into three categories:

- **$E(r_0, \sigma)$ -minimization** [1, 2, 3]. If one simply ignores $Z(\sigma)$ in Eq. (1), one is left with the problem of minimizing $E(r_0, \sigma)$. This is too crude, since for many coarse-grained models it implies that all σ values line up to a homopolymer solution. This can be remedied by adding a constraint to $E(r_0, \sigma)$ restricting the overall composition. This method is very fast since no exploration of the conformation space is involved, but it does fail for a number of examples even for small system sizes.
- **High- T expansion** [4, 5, 6]. A more systematic approach is to approximate $Z(\sigma)$ with low-order terms in a cumulant or high- T expansion. This method is also fast, and slightly more accurate than the $E(r_0, \sigma)$ -minimization method, but can also fail since folding takes place at low T .
- **Nested MC (NMC)** [7]. In order to avoid introducing uncontrolled approximations, one is forced to turn to Monte Carlo (MC) methods. The most straightforward MC approach is to use a normal fixed- σ MC in r for estimating the $Z(\sigma)$ contribution to Eq. (1), which, however, leads to a nested algorithm with a highly non-trivial inner part. Although correct results have been reported for toy-sized problems, this approach is inhibitorily CPU time-consuming for larger problem sizes.

In this paper we develop and explore an alternative MC methodology, **Multisequence (MS)** design, where the basic strategy is to create an enlarged configuration space; the sequence σ becomes a dynamical variable [8]. Hence, r and σ are put on a more equal footing, which, in particular, enables us to avoid a nested MC. Early stages of this project were reported in [9].

The multisequence approach is explored on both a two-dimensional (2D) lattice model, the HP model of Lau and Dill [10], and a simple three-dimensional (3D) off-lattice models [11], with very good results. As with any design method, one needs access to suitable target structures, and also to verify the results by folding calculations. For short chains in the 2D HP model, $N \leq 18$, both these tasks are easy since all configurations can be enumerated. For longer lattice chains and off-lattice models powerful MC algorithms like simulated tempering [12, 13, 8] are needed for the verification.

Our calculations for the HP model can be divided into two groups corresponding to short ($N = 16$ and 18) and long ($N = 32$ and 50) chains. The results for short chains are compared to exact enumerations, and we find that our method reproduces the exact results extremely rapidly. We also compare our results to those obtained by $E(r_0, \sigma)$ -minimization and a high- T approach. It should be mentioned that for the former we scan through all possible fixed overall compositions, thereby giving this method a fair chance. Also, we make a detailed exact calculation illuminating the limitations of the high- T expansion approach.

For larger N a “bootstrap” method is developed that overcomes the problem of keeping all possible sequences in the computer memory. The efficiency of this trick is illustrated for a $N = 32$ target structure, which is chosen “by hand”. Finally, a $N = 50$ target structure is generated by using a design algorithm that aims at throwing away those sequences that are unsuitable for *any* structure. This $N = 50$ target structure is subsequently subject to our multisequence design approach, which readily finds a sequence with the target structure as its unique ground state.

As a by-product, having access to good $N = 50$ sequences, we take a look at the behavior at the folding transition which, to our knowledge, has not been studied before for comparable chain lengths. In terms of an overlap histogram, we find an unambiguous sign of cooperativity. This is in contrast to the general belief that 2D models do not exhibit cooperativity [14].

Earlier studies of the 3D off-lattice model [11], and a similar 2D model [15], have shown that the stability, as measured by the average size $\langle \delta^2 \rangle$ of thermal structural fluctuations, is strongly sequence dependent. Here we perform design experiments using native structures of both stable (low $\langle \delta^2 \rangle$) and unstable (high $\langle \delta^2 \rangle$) sequences as target structures. The quality of the designed sequences is carefully examined by monitoring the thermal average of the mean-square distance to the target structure, $\langle \delta_0^2 \rangle$. We find that the method consistently improves on $\langle \delta_0^2 \rangle$ and that it performs better than the $E(r_0, \sigma)$ -minimization approach.

This paper is organized as follows. Section 2 contains our multisequence approach together with implementation issues. In Sec. 3 the method is applied to the 2D HP model for sizes varying from $N = 16$ to 50. In this section, also comparisons between the different approaches are performed. The efficiency of the multisequence method is discussed in Sec. 4. In Sec. 5 3D off-lattice model structures are designed, and Sec. 6 contains a brief summary.

2 The Method

2.1 Optimizing Conditional Probabilities

Maximizing the conditional probability $P(r_0|\sigma)$ of Eq. (1) with respect to σ for a given target structure r_0 is a challenge since it requires exploration of both conformation and sequence degrees of freedom. At high T this task can be approached by using a cumulant expansion of $Z(\sigma)$, which makes the problem much easier. Unfortunately, this is not the temperature regime of primary interest. In this paper we present an efficient MC-based procedure for sequence optimization at biologically relevant temperatures.

The problem of maximizing $P(r_0|\sigma)$ can be reformulated in terms of $P(\sigma|r_0)$ by introducing a marginal distribution of σ , $P(\sigma)$, and the corresponding joint distribution $P(r,\sigma) = P(r|\sigma)P(\sigma)$. Assigning equal a priori probability to all the σ , i.e. $P(\sigma) = \text{constant}$, one obtains

$$P(r_0|\sigma) = \frac{P(\sigma|r_0)P(r_0)}{P(\sigma)} \propto P(\sigma|r_0), \quad (3)$$

so maximizing $P(r_0|\sigma)$ is then equivalent to maximizing $P(\sigma|r_0)$.

In this paper we focus on the problem of designing a single structure r_0 . This is a special case of the more general problem of maximizing the probability

$$\sum_{r \in D} P(r|\sigma) \quad (4)$$

for a group of desired structures, D . Note that for a general set D with more than one structure, this is not equivalent to maximizing $\sum_{r \in D} P(\sigma|r)$, since

$$\sum_{r \in D} P(r|\sigma) = \sum_{r \in D} \frac{P(\sigma|r)P(r)}{P(\sigma)} \not\propto \sum_{r \in D} P(\sigma|r). \quad (5)$$

Note that Eq. (5) differs from that of [4], where equivalence is assumed.

2.2 The Multisequence Method

A MC-based method for optimization of $P(r_0|\sigma)$ at general T has been proposed by Seno *et al.* [7]. Their approach is based on simulated annealing in σ with a chain-growth MC in r for each σ . This gives a nested MC which is prohibitively time-consuming except for very small systems.

The multisequence method offers a fundamentally different approach. In this method one replaces the simulations of $P(r|\sigma)$ for a number of different fixed σ by a single simulation of the joint probability distribution

$$P(r,\sigma) = \frac{1}{Z} \exp[-g(\sigma) - E(r,\sigma)/T], \quad (6)$$

$$Z = \sum_{\sigma} \exp[-g(\sigma)]Z(\sigma). \quad (7)$$

The parameters $g(\sigma)$ determine the marginal distribution

$$P(\sigma) = \frac{1}{Z} \exp[-g(\sigma)] Z(\sigma) \quad (8)$$

and must therefore be chosen carefully. At first sight, it may seem that one would need to estimate $Z(\sigma)$ in order to obtain reasonable $g(\sigma)$. However, a convenient choice is

$$g(\sigma) = -E(r_0, \sigma)/T, \quad (9)$$

for which one has

$$P(r_0|\sigma) = \frac{P(r_0, \sigma)}{P(\sigma)} = \frac{1}{Z P(\sigma)}. \quad (10)$$

In other words, maximizing $P(r_0|\sigma)$ is in this case equivalent to minimizing $P(\sigma)$. This implies that bad sequences are visited more frequently than good ones in the simulation. This property may seem unattractive at a first glance. However, it can be used to eliminate bad sequences. The situation is illustrated in Fig. 1.

The idea of using the multisequence method for sequence design is natural since the task is to compare different sequences. Let us therefore stress that the method is not only convenient, but also efficient. The basic reason for this is that the system often can move more efficiently through conformation space if the sequence degrees of freedom are allowed to fluctuate. As a result, simulating many sequences with the multisequence method can be faster than simulating a *single* sequence with standard methods, as will be shown in Sec. 4. Another appealing feature of the multisequence scheme is that the optimization of the desired quantity $P(r_0|\sigma)$, which refers to a single structure, can be replaced by an optimization of the marginal probability $P(\sigma)$.

The basic idea of the multisequence method is the same as in the method of simulated tempering [12, 13, 8]. The only difference is that in the latter it is the temperature rather than the sequence which is dynamical. It has been shown that simulated tempering is a very efficient method for fixed-sequence simulations in the HP model [16]. In particular, it was applied to a $N = 64$ sequence with known ground state, for which other methods had failed to reach the ground state level. Simulated tempering was, by contrast, able to find the ground state. Below we use simulated tempering to check our sequence design results for long chains.

2.3 Reducing the Sequence Set

The simple scheme outlined above is normally of little use on its own. With a large number of sequences, it becomes impracticable, especially since bad sequences tend to dominate in the simulation. It is therefore essential to incorporate a procedure for removal of bad sequences. This elimination can be done in different ways. We will discuss two possibilities which will be referred to as $P(\sigma)$ - and $E(r, \sigma)$ -based elimination, respectively. Whereas both options are available for lattice models, $P(\sigma)$ -based elimination is more appropriate for off-lattice models.

2.3.1 $P(\sigma)$ -Based Elimination

$P(\sigma)$ -based elimination relies on the fact that bad sequences have high $P(\sigma)$ [see Eq. (10)]. The full design procedure consists in this case of a number of ordinary multisequence runs. After each

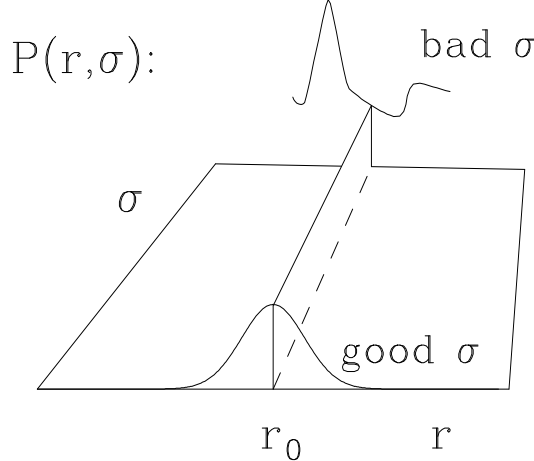


Figure 1: The distribution $P(r, \sigma)$. The choice of $g(\sigma)$ in Eq. (9) makes $P(r_0, \sigma)$ flat in σ . A sequence not designing r_0 will have maxima in $P(r_i|\sigma)$ for $r_i \neq r_0$ due to states with $E(r_i, \sigma) \leq E(r_0, \sigma)$. A sequence designing r_0 will have a unique maximum at $r = r_0$ in $P(r|\sigma)$, which for low T contains most of the probability.

of these runs $P(\sigma)$ is estimated for all the N_r remaining sequences, and those having

$$P(\sigma) > \Lambda/N_r \quad (11)$$

are removed. Typical values of the parameter Λ are 1–2.

2.3.2 $E(r, \sigma)$ -based Elimination

The procedure referred to as $E(r, \sigma)$ -based removes sequences that do not have the target structure r_0 as their unique ground state. For each conformation $r \neq r_0$ visited in the simulation, it is checked, for each remaining sequence σ , whether

$$E(r, \sigma) \leq E(r_0, \sigma). \quad (12)$$

Those sequences for which Eq. (12) is true are removed. With this type of elimination, it may happen that one removes the sequence that actually maximizes $P(r_0|\sigma)$ at the design temperature — the best sequence at this temperature does not necessarily have r_0 as its unique ground state (for an example, see Fig. 4 below). This should not be viewed as a shortcoming of the method. If it happens, it rather means that the design temperature is too high. $E(r, \sigma)$ -based elimination is free from statistical errors in the sense that a sequence that does have r_0 as its unique ground state cannot be removed. Hence, in a very long simulation the surviving sequences are, by construction, precisely those that have r_0 as their unique ground state.

2.4 Restricted Search by Clamping

For long chains it is not feasible to explore the entire sequence space. On the other hand, at least in a hydrophobic/hydrophilic model, there are typically several positions in the target structure where σ_i is effectively frozen (see e.g. [17, 18]). As will be discussed below, it turns out that such positions can be easily detected by means of trial runs.

3 Lattice Model Results

In this section we explore the multisequence approach on the HP model on the square lattice. In this context we also compare with and discuss other approaches; $E(r_0, \sigma)$ -minimization and high- T expansions.

The HP model contains two monomer types, H (hydrophobic) and P (hydrophilic/polar), and is defined by the energy function [10]

$$E(r, \sigma) = - \sum_{i < j} \sigma_i \sigma_j \Delta(r_i - r_j), \quad (13)$$

where $\Delta(r_i - r_j) = 1$ if monomers i and j are non-bonded nearest neighbors and 0 otherwise. For hydrophobic and polar monomers, one has $\sigma_i = 1$ and 0, respectively.

Our explorations naturally divide into two categories; $N = 16$ and 18, where finding suitable structures and verifying folding properties of the designed sequences is trivial, and $N = 32$ and 50, where this is not the case.

For $N \leq 18$ the HP model can be solved exactly by enumeration. Hence such systems have been extensively used for gauging algorithm performances. In Table 1 properties for $N = 16$ and 18 systems are listed [19, 20]. A structure is designable if there is some sequence that has it as its unique ground state. One should mention that the fraction of designable structures drops sharply with N . Furthermore, it depends strongly upon local interactions, as was demonstrated in [20].

For a given target structure r_0 , it is convenient to classify the sequences as “good”, “medium” or “bad”. *Good* sequences have r_0 as their unique ground state, whereas *medium* sequences have $g > 1$ degenerate ground states, one of them being r_0 . Finally, *bad* sequences do not have r_0 as minimum energy structure.

In our calculations below for the HP model, the elementary moves in r space are standard. The new feature is that these are combined with stochastic moves in σ . Throughout our HP model calculations a “sweep” refers to a combination of r and σ updates as described in the Appendix.

3.1 N=16/18

We have performed design calculations for a large number of different $N = 16$ and 18 target structures, using multisequence $E(r, \sigma)$ -based elimination. In Figs. 2a,b we show two target structures

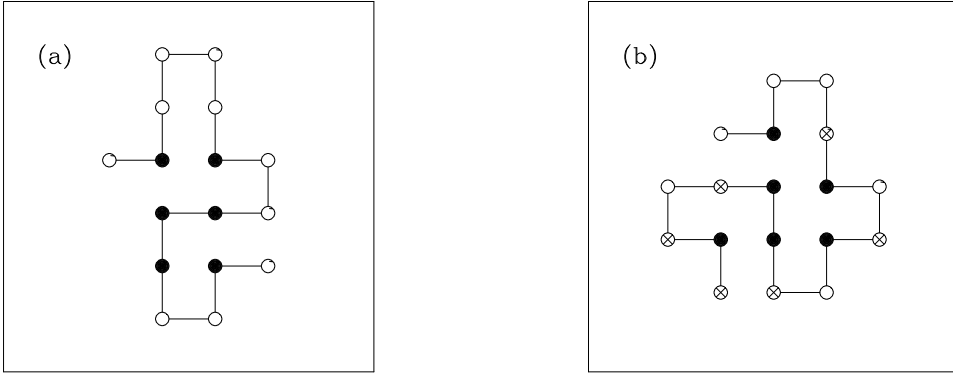


Figure 2: **(a)** Target structure for $N = 16$. There is only one good sequence for this structure. Full and open circles correspond to H and P, respectively, for this sequence. **(b)** Target structure for $N = 18$. For this structure there are seven good sequences. Full and open circles indicate positions where all these seven sequences have the same monomer type, H and P, respectively. Positions where σ_i varies among the good sequences are represented by crosses.

that are used as examples.

Since the elimination is $E(r, \sigma)$ -based, only the good sequences survive if the simulation is sufficiently long. For a wide variety of target structures, we measured the number of MC sweeps it takes to remove all of the medium and bad sequences, when starting from all 2^N possible sequences. For the $N = 16$ example in Fig. 2a, there is one good sequence. After 8000 MC sweeps, corresponding to a few CPU seconds on a DEC Alpha 200, all sequences except the correct one had been removed.

To check that this was not due to a lucky choice of target structure, the experiment was repeated for all 1475 designable $N = 18$ structures, starting with five different seeds for each structure. The average number of MC sweeps needed to single out the good sequences for each target structure was 123000 (30 CPU seconds). A very few experiments required up to 10^7 MC sweeps, while all five experiments converged in less than 500000 MC sweeps for 90% of the structures. This shows that the elimination procedure is both fast and robust.

Those sequences that survive the elimination are then compared by determining their relative weights $P(\sigma)$, see Eq. (10). As an example, we show in Table 2 the results obtained for the $N = 18$ structure in Fig. 2b, for which there are seven good sequences. Shown are both the MC results and the exact ones.

	$N = 16$	$N = 18$
# of sequences (2^N)	65 536	262 144
# of sequences with unique ground state	1 539	6 349
# of structures	802 075	5 808 335
# of designable structures	456	1 475

Table 1: Sequence and structure statistics for the HP model for $N = 16$ and 18.

Sequence	$P(\sigma)$		$P(r_0 \sigma)$	
	MS	exact	MS	exact
PHPPPHPPHPPHHPPPH	0.2101 ± 0.0008	0.2112	0.0175 ± 0.0005	0.0175
PHPPHHPPHPPHHPPPH	0.0625 ± 0.0009	0.0617	0.0599 ± 0.0017	0.0599
PHPPPHPPHPPHHPPPH	0.3104 ± 0.0018	0.3112	0.0120 ± 0.0003	0.0119
PHPPPHPPHPPHHPPPH	0.0495 ± 0.0003	0.0495	0.0748 ± 0.0020	0.0747
PHPPPHPHPPHHPPPH	0.1765 ± 0.0019	0.1757	0.0211 ± 0.0006	0.0210
PHPPPHPPHPPHHPPPH	0.1102 ± 0.0007	0.1110	0.0333 ± 0.0010	0.0333
PHPPPHPPHPPHHPPPH	0.0807 ± 0.0019	0.0797	0.0473 ± 0.0017	0.0464

Table 2: $P(\sigma)$ and $P(r_0|\sigma)$ for the seven $N = 18$ sequences that design the structure shown in Fig. 2b. Listed are both the results from our multisequence simulation (MS) and the exact results from complete enumeration, for $T = 1/3$.

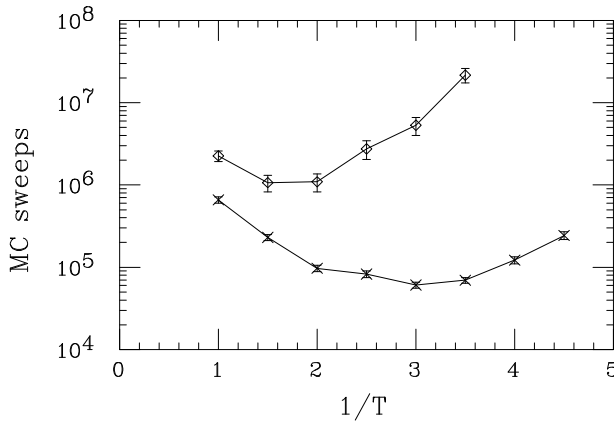


Figure 3: The number of MC sweeps needed to single out the seven good sequences for the structure in Fig. 2b when using $E(r, \sigma)$ -based elimination. Each data point represents an average over 50 experiments, each started from the full set of all 2^{18} sequences. Shown are both results obtained with (\times) and without (\diamond) stochastic sequence moves.

The stochastic σ moves are essential in the second part of these calculations, when estimating $P(\sigma)$, but the first part, $E(r, \sigma)$ -based elimination, could in principle be done without using these moves. In this case, if the simulated sequence is to be removed, it can be replaced by a randomly chosen sequence among the remaining ones. It turns out, however, that it is advantageous to include the stochastic σ moves in the first part as well. To illustrate this, we show in Fig. 3 results obtained both with and without these moves, for the target structure in Fig. 2b. The results show that the number of MC sweeps required to remove all medium and bad sequences can be reduced by more than a factor of 10 by including the stochastic σ moves. Furthermore, it can be seen that the efficiency is less T dependent in this case.

3.2 Other Methods

In this section we briefly discuss two alternative methods, $E(r_0, \sigma)$ -minimization and high- T expansions, together with a comparison of the results.

3.2.1 Minimizing $E(r_0, \sigma)$

Maximizing $P(r_0|\sigma)$ [see Eq. (1)] is equivalent to minimizing the quantity

$$\Delta F_0(\sigma) = -T \ln P(r_0|\sigma) = E(r_0, \sigma) - F(\sigma), \quad (14)$$

where $F(\sigma)$ is the free energy of sequence σ at temperature T . In the energy minimization method [2], one approximates $\Delta F_0(\sigma)$ by replacing $F(\sigma)$ with a constraint that conserves the net hydrophobicity to a preset value N_H ,

$$\sum_i \sigma_i = N_H. \quad (15)$$

For small systems this constraint is enforced exactly, whereas for larger systems it is implemented softly with a penalty term added to E . The reason for imposing this constraint is more fundamental than just guiding the sequence optimization to an appropriate net hydrophobicity. In e.g. the HP model one has a pure “ferromagnetic” system in terms of σ_i for a fixed r_0 . Hence, minimizing $E(r_0, \sigma)$ with respect to σ would result in a homopolymer with all monomers being hydrophobic. With the constraint in Eq. (15) present, this is avoided.

In [2] the relevant N_H is picked for the structure to be designed. However, this does not correspond to a “real-world” situation, where only the structure and not N_H is known beforehand. When comparing algorithm performances in [5, 7] a default constraint, $N_H = N/2$, was therefore used. Below, we will in our comparisons scan through all N_H and minimize $E(r_0, \sigma)$ separately for each N_H .

For $N = 16$ and 18 all 456 respective 1475 different *designable* structures (see Table 1) are subject to design by minimizing $E(r_0, \sigma)$ for all N_H . If the resulting minima are non-degenerate for fixed N_H , the sequences are kept as candidates for good sequences, otherwise they are discarded. A check of the results obtained this way against exact data shows that there is at least one good sequence among the candidates for 87% ($N = 16$) and 78% ($N = 18$) of the structures. In these cases we say that the method successfully can design the structure. Another measure of the success of the method is given by the probability that an arbitrary generated candidate is good. In total, we obtained 939/3546 candidates for $N = 16$ and 18 , respectively, out of which 46%/36% (435/1245 sequences) are good. Therefore, in order to get the relatively high success rates mentioned above, it is essential to be able to distinguish good candidates from bad ones. The cost of doing this is for long chains much larger than that of the energy minimization itself.

In Table 3 the performance of the $E(r_0, \sigma)$ -minimization methods for $N = 16$ and 18 is compared with other approaches with respect to design ability and CPU consumption. As can be seen, the multisequence method with its 100% performance, is indeed very fast. Furthermore, the performance of the $E(r_0, \sigma)$ -minimization variants deteriorates with size.

	$E(r_0, \sigma)$ -minimization		High- T	NMC	MS
	$N_H = N/2$	All N_H			
HP $N = 16$	25%	87%	70%	100%	100%
HP $N = 18$	21%	78%	50%	100%	100%
CPU sec/structure	$O(0.1)$	$O(1)$	$O(0.1)$	$O(10^3)$	$O(10)$

Table 3: Number of structures that get designed by the different approaches for $N = 16$ and 18 in the HP model; $E(r_0, \sigma)$ -minimization with fixed $N_H = N/2$ and with scanning through all N_H , respectively, the nested MC approach of [7] (NMC), and the multisequence method (MS). Also shown is the computational demand for $N = 18$ (DEC Alpha 200).

3.2.2 High- T Expansion – Crossings

A more systematic approach, based on cumulant approximations of $F(\sigma)$, has been advocated by Deutsch and Kuroska [5], and a method along these lines has also been proposed by Morrissey Shakhnovich [6]. However, these are high- T approximations, and can fail at relevant design temperatures, as has been pointed out by Seno *et al.* [7].

The importance of the choice of the design temperature is easily studied for short HP chains, for which the T dependence of $P(r_0|\sigma)$ can be computed exactly. At $T = 0$ the relative population of r_0 , $P(r_0|\sigma)$, is equal to 1, $1/g$, and 0 for good, medium, and bad sequences, respectively. Note that stability in the sense that $P(r_0|\sigma) > 1/2$, cannot be obtained at any T for any medium or bad sequence. For good sequences, the temperature at which $P(r_0|\sigma) = 1/2$ is often referred to as the folding temperature.

We calculated the T dependence of $P(r_0|\sigma)$ for the two target structures that are shown in Fig. 2. The $N = 16$ structure (a) from [7] has 1 good and 1322 medium sequences, whereas the $N = 18$ structure (b) from [9] has 7 good and 2372 medium sequences. In the $N = 18$ case, it turns out that there are 667 medium sequences that have higher $P(r_0|\sigma)$ than at least one of the good sequences at some T . We denote these as *crossing* sequences. Figure 4 shows the results for the 7 good sequences and 4 of the crossing sequences. In particular, one sees that in order for $P(r_0|\sigma)$ optimization to actually lead to a good sequence, it is necessary to work at a design temperature not much higher than the highest folding temperature. At such low temperatures, it is clear that high- T approximations are inappropriate.

For the $N = 16$ structure it was demonstrated in [7] that the method of [5] fails. Indeed, it turns out that this structure has 296 crossing sequences.

With these crossing phenomena, it is not surprising that the high- T expansion frequently fails as can be seen from the summary in Table 3, from which it is also clear that the performance deteriorates when increasing N from 16 to 18.

MC methods has the advantage that the design temperature can be taken low enough to avoid crossing problems, without introducing any systematic bias. Still, in practise, it is of course not possible to work at too low design temperatures, due to long decorrelation times at low T . It is therefore important to note that the multisequence $E(r, \sigma)$ -based elimination multisequence method can be carried out at any temperature without running the risk of eliminating any good sequences.

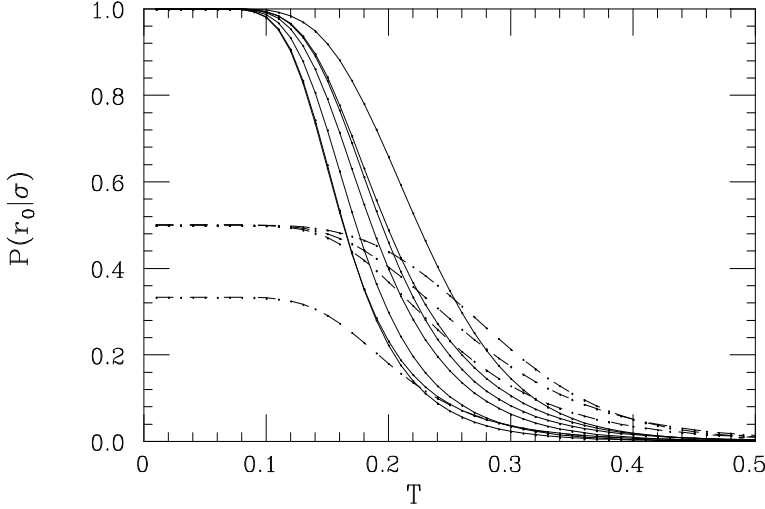


Figure 4: $P(r_0 | \sigma)$ versus T for the seven good sequences (solid) and for four of the crossing sequences (dashed) for the structure in Fig. 2b.

3.3 $N=32$

Having compared different methods for short chains, we now turn to longer chains focusing on multisequence design. For long chains it is not feasible to explore the entire sequence space. On the other hand, it is expected that, for a given target structure, there are several positions along the chain where most of the good sequences share the same σ_i value (see e.g. [17, 18]); in other words, some positions are effectively frozen to H or P. A natural approach therefore is to restrict the search by identifying and subsequently clamping such σ_i to H or P.

In order to determine which σ_i to clamp, it is convenient to use a set of short trial runs. To illustrate this, we consider the $N = 32$ target structure in Fig. 5a. For this target structure we performed ten trial runs, using $E(r, \sigma)$ -based elimination. Each of these runs was started with a set of 10^5 random sequences. After 20000 MC sweeps between 15 and 57 sequences remained, and for these surviving sequences the average σ_i was calculated. The σ_i profile obtained this way is shown in Fig. 5b, from which it is clear that many σ_i indeed exhibit a clear preference for either P ($\sigma_i = 0$) or H ($\sigma_i = 1$). Based on this, we divide the positions along the chain into three groups corresponding to $\sigma_i > \sigma^{(1)}$ (filled circles in Fig. 5a), $\sigma_i < \sigma^{(2)}$ (open circles) and $\sigma^{(2)} < \sigma_i < \sigma^{(1)}$ (crosses), as indicated in Fig. 5b. Sequence optimization is then performed with those σ_i in the first two groups clamped to H or P, and those in the third group left open (crosses). It turns out that this restricted set of 2^{12} sequences indeed contains a number of good sequences.

This clamping method can of course be generalized to a corresponding multi-step procedure for very long chains.

Next we compare the efficiency of $E(r, \sigma)$ -based elimination to that of $P(\sigma)$ -based elimination using the target structure in Fig. 5a with the search restricted to 2^{12} sequences as described above. In Fig. 6 we show the number of remaining sequences, N_r , against MC time in three runs for each of

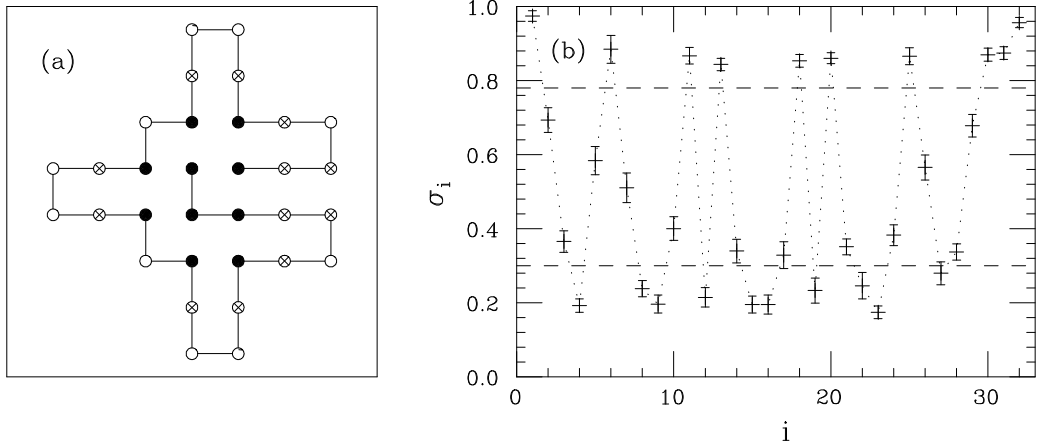


Figure 5: (a) Target structure for $N = 32$. Symbols are explained in the text. (b) Average of σ_i against i for the surviving sequences from 10 runs for this target structure, each started with a set of 10^5 random sequences. The upper and lower lines represent $\sigma^{(1)}$ and $\sigma^{(2)}$, respectively (see text).

the two methods ($T = 1/3$, 1 CPU hour or less per run). $E(r, \sigma)$ -based elimination is very fast in the beginning, and a level is quickly reached at which it is easy to perform a final multisequence simulation for the remaining sequences. The curves level off at relatively high N_r , indicating that there are many good sequences for this structure (these runs were continued until all three contained the same 167 sequences). The three runs with $P(\sigma)$ -based elimination, which were carried out using 50000 MC sweeps for each elimination step and $\Lambda = 2$ [see Eq. (11)], were continued until five sequences or fewer were left. The results were checked against those of the long multisequence simulations discussed in Sec. 4, and were found to be quite stable in spite of the fact that the runs were short. In particular, the best sequence (sequence A of Table 4 below) was among the survivors in all three cases.

The performance of the design procedure is crucially dependent on the shape of the distribution $P(\sigma)$. In particular, this is the case when $P(\sigma)$ -based elimination is used. One runs into problems if this distribution is dominated by a relatively small number of sequences with high $P(\sigma)$. It is therefore interesting to see how the shape of $P(\sigma)$ evolves as the elimination process proceeds. Figure 7a shows the entropy of $P(\sigma)$,

$$H = - \sum_{\sigma} P(\sigma) \log_2 P(\sigma), \quad (16)$$

in a run with $P(\sigma)$ -based elimination for the $N = 32$ structure in Fig. 5a. With N_r remaining sequences, the maximal value of H is $\log_2 N_r$, corresponding to a uniform distribution $P(\sigma)$. As can be seen from Fig. 7a, after a few elimination steps, H is close to this limit. The desired behavior of the marginal distribution of r , $P(r)$, is in a sense the opposite, since the weight of the target structure should become large. The evolution of $P(r_0)$ in the same run is shown in Fig. 7b.

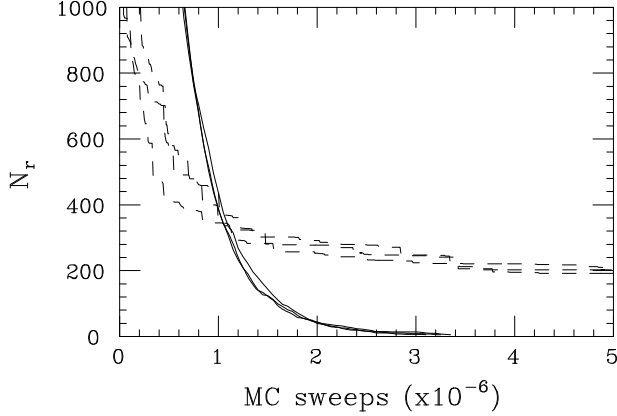


Figure 6: The number of remaining sequences, N_r , against MC time for three runs with $P(\sigma)$ -based elimination (full lines) and three with $E(r, \sigma)$ -based elimination (dashed lines) for the target structure in Fig. 5a. Each run was started from the set of 2^{12} sequences obtained when leaving open those σ_i that correspond to crosses in Fig. 5a.

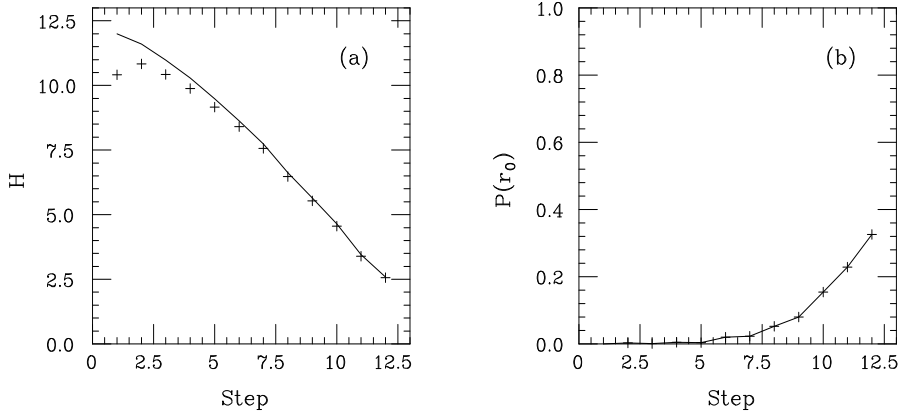


Figure 7: The evolution of (a) the entropy of $P(\sigma)$ and (b) the marginal probability $P(r_0)$ in a run with $P(\sigma)$ -based elimination ($T = 1/3$, $\Lambda = 1$, 10^7 MC sweeps for each elimination step) for the target structure in Fig. 5a. The line in (a) shows $\log_2 N_r$, where N_r is the number of remaining sequences. After twelve elimination steps there were two sequences left.

3.4 N=50

A test of any design procedure consists of three steps:

1. Finding a suitable target structure.
2. Performing the actual design.
3. Verifying that the final sequence is good.

In this section we discuss the design of a $N = 50$ structure. For this system size the first step is

highly non-trivial. Also, the verification part is quite time-consuming. For these reasons we focus on one example and go through each of the steps in some detail.

3.4.1 Finding a Suitable Target Structure

We begin with the problem of finding a suitable target structure. For a randomly chosen structure it is unlikely that there is any sequence that can design it; the fraction of designable structures is e.g. about 0.00025 for $N = 18$ (see Table 3). Furthermore, this fraction decreases with system size. Rather than proceeding by trial and error, we therefore determined the target structure by employing a variant of our sequence design algorithm. In this version no target structure is specified and Eq. (9) is replaced by

$$g(\sigma) = -E_{\min}(\sigma)/T, \quad (17)$$

where $E_{\min}(\sigma)$ ideally should be the minimum energy for the sequence σ . In our calculations, since the minimum energy is unknown, we set $E_{\min}(\sigma)$ equal to the lowest energy encountered so far. Except for this change of the parameters $g(\sigma)$, we proceed exactly as before, using $P(\sigma)$ -based elimination. However, a sequence is never eliminated if its $g(\sigma)$ was changed during the last multisequence run, that is if a new lowest energy was found during this run.

With this algorithm, one may hope to identify and eliminate those sequences that are bad not only with respect to one particular structure, but with respect to all possible structures. Clearly, this is a much more ambitious goal, and it should be stressed a careful evaluation of the usefulness of this approach is beyond the scope of the present paper. Here we just want to outline the calculation that gave us our $N = 50$ target structure.

This calculation was started from a set of about 2200 sequences. These were obtained by first randomly generating a mother sequence, with probability 0.65 for H, and then randomly changing this at one or two positions. Thus, there is a high degree of similarity between the sequences, which ensures a reasonable acceptance rate for the sequence update. After 37 elimination steps ($T = 1/2.8$, $\Lambda = 1.5$, 2×10^5 MC sweeps for each elimination step), three of the sequences were left. The best of these three sequences and its minimum energy structure can be found in Fig. 8. Note that this sequence does not minimize the energy for any fixed N_H — the energy can be reduced by interchanging the monomers $i = 19$ and 43 ($i = 1$ corresponds to the lowest of the two end points in Fig. 8). In what follows we take this structure as our target structure, without using any information about the particular sequence shown.

3.4.2 Sequence Design

We start the sequence design for this structure by applying the clamping procedure. As in the $N = 32$ case, ten relatively short runs were performed, each started from 10^5 random sequences. The results from these runs are summarized in Fig. 9. The classification of the positions along the chain as H, P or open is illustrated in Fig. 9a. It is interesting to compare this pattern to the original sequence in Fig. 8. As expected, there is a close similarity, but there are also three positions along the chain at which σ_i is clamped to the opposite value compared to the original sequence ($i = 2, 19$ and 43). Thus, the original sequence does not belong to the restricted sequence set which we study next.

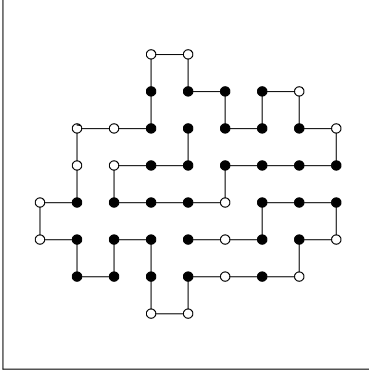


Figure 8: Target structure for $N = 50$. This structure and the sequence shown were obtained using the design algorithm without fixed target [see Eq. (17)].

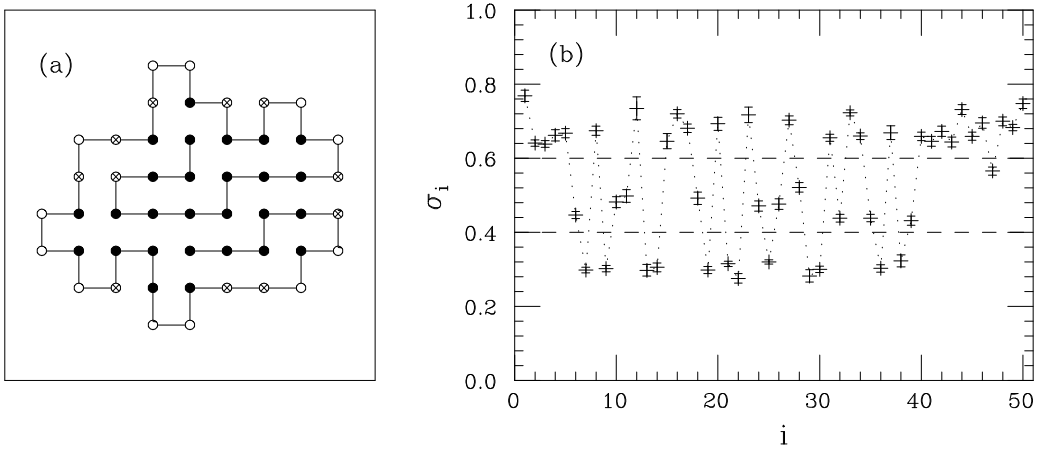


Figure 9: Results of the clamping procedure for our $N = 50$ target structure. Symbols are the same as in Fig. 5. The data in (b) are averages over ten runs, each started from 10^5 random sequences and consisting of 40000 MC sweeps. The number of surviving sequences varied between 114 and 368.

For the sequence set obtained by clamping (see Fig. 9a), we proceed in two steps. First, we apply $E(r, \sigma)$ -based elimination. As in the corresponding $N = 32$ calculation, the number of remaining sequences rapidly reached a fairly stable and high level, indicating that there are many sequences with the target structure as unique ground state. The number of sequences surviving this first step was 832. The second step is a simulation with $P(\sigma)$ -based elimination ($T = 1/2.8$, $\Lambda = 1$, 10^7 MC sweeps for each elimination step). This step was repeated three times using different random number seeds, each time starting from the same 832 sequences. The stability of the results was not perfect, but the best sequence found was the same in all three runs. This sequence has four H and seven P at the eleven positions that were left open after clamping. The four positions that were assigned the value H are $i = 10, 11, 18$ and 28.

3.4.3 Verification

In order to check the designed sequence, we performed a long independent calculation using the simulated-tempering method. As mentioned in Sec. 2.2, in a previous study [16], this method successfully found the ground state of a $N = 64$ HP chain [16]. The length of our $N = 50$ simulation is 2×10^9 MC sweeps, which is slightly longer than for this $N = 64$ simulation.

In the simulation of the designed $N = 50$ sequence the target structure was visited many times; we estimate the number of “independent” visits to be about 30. By contrast, no other structure with the same or lower energy was encountered. We take this as strong evidence that the target structure indeed is a unique energy minimum for this sequence.

Similar simulations were also performed for two other $N = 50$ sequences, to be called S1 and S2. The sequence S1 is the one shown in Fig. 8, and S2 is the one obtained by assigning P to all open positions in Fig. 9a. At first sight S1 may not seem to fit the target structure very well; as already noticed, this sequence does not minimize the energy of the target structure for fixed N_H . Nevertheless, our results suggest that both S1 and S2, like the designed sequence, have the target structure as unique ground state. However, the dominance of this structure sets in at a lower temperature for S1 and S2 than for the designed sequence; rough estimates of the folding temperatures are 0.27 for the designed sequence and 0.23 for S1 and S2.

Unfortunately, it was not feasible to evaluate alternative methods for this system size, because the verification part is too time-consuming. Let us note, however, that our designed sequence uniquely minimizes the energy of the target structure for fixed $N_H = 31$. On the other hand, there are also good sequences, for example S2, that do not minimize the target energy for any N_H .

3.5 The Folding Transition for $N=50$

We have here, for convenience, used a two-dimensional model as test bed for our sequence design procedure. An important argument against such models [14] is that the folding transition is expected to be gradual rather than cooperative in two dimensions. This expectation is based on general arguments [21]. Previous numerical studies (see e.g. [22]) have, however, been limited to relatively short chains. Let us therefore see how the $N = 50$ sequences of the previous section behave at the folding transition.

A standard observable when studying the folding transition is the similarity parameter Q , which measures the number of contacts that a given conformation share with the native state. The $N = 50$ target structure contains 34 contacts, so the maximum possible $Q = Q_{\max} = 34$ for our sequences. In Fig. 10 we show the probability distribution of Q close to the folding transition both for the designed sequence and the sequence S2 (see Sec. 3.4.3). The peaks at $Q = 34$ correspond to the native state, that is the target structure. For both sequences, it can be seen that there is a significant population of states with $Q/Q_{\max} = 0.4 - 0.6$, while there are higher Q where $P(Q)$ is suppressed. This immediately shows that the folding transition is not a simple gradual process for these sequences.

On the other hand, it is also not a simple two-state process where the non-native state corresponds to extended, more or less coil-like conformations. This can be seen from the distributions of energy

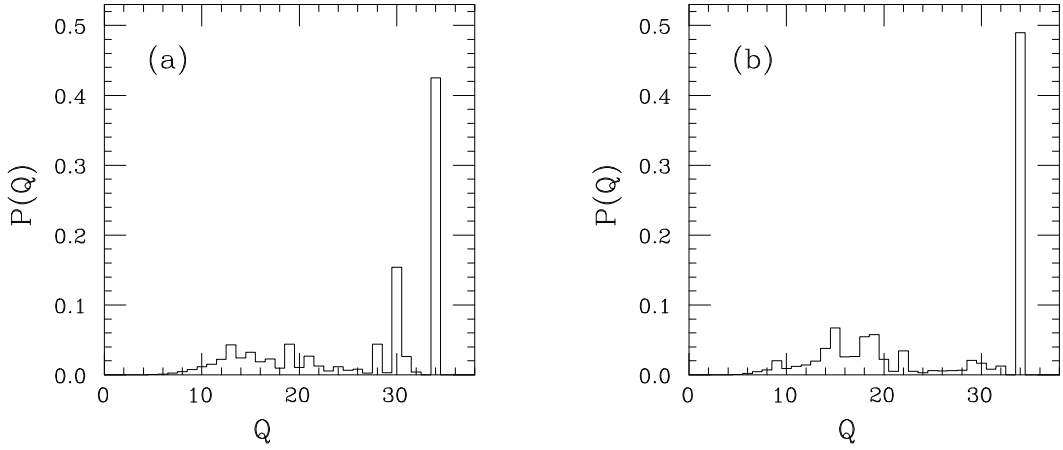


Figure 10: The probability distribution of the similarity parameter Q near the folding transition for two $N = 50$ sequences: (a) the designed sequence ($T \approx 0.285$), and (b) the sequence S2 ($T \approx 0.227$).

and the total number of contacts, which both have a single peak. A more accurate picture appears to be that the thermodynamic behavior is dominated by a limited number of distinct compact low-energy states. These states may or may not be similar to the native state. For the designed sequence there exist other contributing states that are similar to the native state, as can be seen from the presence of the two peaks at $Q = 28$ and 30 . For the sequence S2 such states are missing, which leads to an essentially bimodal distribution of Q .

The results discussed here refer to a single target structure and it is, of course, difficult to say how representative they are. However, they do show that long chains display properties that make it necessary to interpret results obtained for short chains with care. This in turn underlines the importance of improved computational methods.

4 The Multisequence Method

The multisequence method, which is a key ingredient in our design algorithm, was originally applied to a simple off-lattice model [8] in the context of folding studies. Using parameters $g(\sigma)$ that had been adjusted so as to have an approximately uniform distribution in σ , it was found to be much more efficient than a standard MC. In this paper we have instead chosen $g(\sigma)$ according to Eq. (9). This simple choice is not possible for a random set of sequences. The efficiency can, however, be quite good after removal of bad sequences. To illustrate this, we take a set of 180 surviving $N = 32$ sequences, from one of the three runs with $E(r, \sigma)$ -based elimination in Fig. 6.

For these sequences we carried out multisequence simulations at three different temperatures, $T=1/2.8, 1/3.1$ and $1/3.4$. The results of these simulations are compared to those of single-sequence simulations with identical r updates, for the three different sequences shown in Table 4. Sequence A is the best sequence found among all the 180. As can be seen from Table 5, it has a folding temperature close to $T = 1/3.1$. Sequences B and C were deliberately chosen to represent different

Sequence A	HHPP HHPP PPHP HPPP PHPH PPPP HHPP HHHH
Sequence B	HHHP HHPP PPHP HPPP PHPH PPPP HHPH HHHH
Sequence C	HHPP HHPP PPHP HPPP PHPH PPPP HHPH PHHH

Table 4: Three $N = 32$ HP sequences.

		$1/T = 2.8$	$1/T = 3.1$	$1/T = 3.4$
Sequence A	Standard MC	0.227 ± 0.005	0.532 ± 0.010	0.752 ± 0.015
	Multisequence	0.234 ± 0.006	0.520 ± 0.010	0.732 ± 0.008
Sequence B	Standard MC	0.0389 ± 0.0024	0.086 ± 0.007	0.166 ± 0.021
	Multisequence	0.0383 ± 0.0013	0.095 ± 0.003	0.166 ± 0.006
Sequence C	Standard MC	0.00251 ± 0.00012	0.0066 ± 0.0003	0.0133 ± 0.0008
	Multisequence	0.00250 ± 0.00009	0.0066 ± 0.0003	0.0123 ± 0.0005

Table 5: Comparison of results for $P(r_0|\sigma)$ obtained by two different methods, the multisequence algorithm and a standard fixed-sequence MC. Shown are results for the three sequences in Table 4 for three different temperatures.

types of behavior, and have lower folding temperatures. It is interesting to note how different the sequences A and C behave (see Table 5), in spite of the fact that they differ only by an interchange of two adjacent monomers.

As the number of sweeps is the same, 10^9 , and since the cost of the additional sequence moves in the multisequence runs is negligible, we can directly compare the statistical errors from these runs. In Table 5 the averages and statistical errors for the quantity $P(r_0|\sigma)$ are shown. The errors quoted are 1σ errors, obtained by a jackknife procedure.

From Table 5 it can be seen that the two methods give similar statistical errors at the highest T studied, which lies above the folding temperature for all three sequences. It should be stressed that equal errors implies that the multisequence method is faster by a factor of 180, since a single run covers all sequences with this method. Although there is a dependence upon sequence, there is furthermore a clear tendency that the errors from the multisequence runs get smaller than those from the single-sequence runs at lower T . The difference is largest for sequence B and the lowest temperature. In this case the errors differ by a factor of 3.5, which corresponds to an extra factor of 10 in computer time, in addition to the trivial factor of 180.

This simple choice of $g(\sigma)$ [Eq. (9)] has been used with success in all our calculations. Nevertheless, let us finally note that multisequence design can also be applied using other $g(\sigma)$ values. In particular, it is easy to modify Eq. (10) for general $g(\sigma)$.

5 Off-Lattice Model Results

Lattice models offer computational and pedagogical advantages, but the results obtained on the lattice must be interpreted with care; for example, it is has been shown that the number of designable

structures drastically depends on the lattice type in the HP model [20]. In this section we therefore show that our design procedure can be applied essentially unchanged to a 3D minimalist off-lattice model [11]. While similar models have been studied before, see e.g. [15, 23, 24, 25], it is the first time, as far as we know, that sequence design is performed in an off-lattice model based on sampling of the full conformation space.

One problem encountered in going to off-lattice models is in the very formulation of the stability criterion. Clearly, it is the probability of being in the vicinity of the target structure r_0 that we are interested in, rather than the probability of being precisely in r_0 . While this point can be relevant for lattice models too, it is of more obvious importance in the off-lattice case. Throughout this paper, we stick to the probability $P(r_0|\sigma)$ corresponding to a single target structure r_0 , using target structures that are obtained by energy minimization. In the general case, it might be necessary to consider instead the off-lattice analogue of the left hand side of Eq. (5).

Another problem is the elimination criterion for bad sequences. A straightforward implementation of $E(r_0, \sigma)$ -based elimination requires the introduction of a cutoff in structural similarity to r_0 , below which elimination should not take place. However, with such a cutoff, the method is too slow, since in order to have a reasonable elimination rate, it appears necessary to employ some sort of quenching procedure, which tends to be very time-consuming. By contrast, we found $P(\sigma)$ -based elimination to be useful for off-lattice chains too, without any modifications or additional parameters.

For the off-lattice model in contrast to the HP model, one does not have access to a set of small N exact enumerations results. Hence, for all sizes we need to go through the three steps needed for $N > 18$ HP chains: find suitable structures, perform design and verify that the designed sequence is stable in the desired structure.

5.1 The Model

Like the HP model, the 3D off-lattice model [11] contains two kinds of residues, hydrophobic ($\sigma_i = 1$) and hydrophilic ($\sigma_i = 0$). Adjacent residues are linked by rigid bonds of unit length, \hat{b}_i , to form linear chains. The energy function is given by

$$E(\hat{b}; \sigma) = -\kappa_1 \sum_{i=1}^{N-2} \hat{b}_i \cdot \hat{b}_{i+1} - \kappa_2 \sum_{i=1}^{N-3} \hat{b}_i \cdot \hat{b}_{i+2} + 4 \sum_{i=1}^{N-2} \sum_{j=i+2}^N \epsilon(\sigma_i, \sigma_j) \left(\frac{1}{r_{ij}^{12}} - \frac{1}{r_{ij}^6} \right) \quad (18)$$

where r_{ij} denotes the distance between residues i and j . The first two *sequence-independent* terms define the local interactions, which turn out to be crucial for native structure formation [11]. The parameters are chosen as $\kappa_1 = -1$ and $\kappa_2 = 0.5$ in order to obtain thermodynamically stable structures, and to have local angle distributions and bond-bond correlations that qualitatively resemble those of functional proteins. The third term represents the *sequence-dependent* global interactions modeled by a Lennard-Jones potential. The depth of its minimum, $\epsilon(\sigma_i, \sigma_j)$, is chosen to favor the formation of a core of hydrophobic residues by setting $\epsilon(0, 0) = 1$, $\epsilon(1, 1) = \epsilon(0, 1) = \epsilon(1, 0) = \frac{1}{2}$.

To monitor structural stability we introduce the usual mean-square distance δ_{ab}^2 between two arbitrary configurations a and b ;

$$\delta_{ab}^2 = \min \frac{1}{N} \sum_{i=1}^N |\bar{x}_i^{(a)} - \bar{x}_i^{(b)}|^2, \quad (19)$$

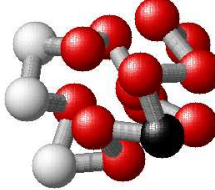


Figure 11: A representative target structure (for sequence 16-1 in Table 6). The hydrophobic and hydrophilic monomers are represented by grey and white spheres, respectively. The mother sequence and the MS-optimized sequence differ only in position 12, which is marked by a black sphere.

where $|\bar{x}_i^{(a)} - \bar{x}_i^{(b)}|$ is the distance between the sites $\bar{x}_i^{(a)}$ and $\bar{x}_i^{(b)}$, and where the minimum is taken over translations, rotations and reflections. An informative measure of structural stability is given in terms of the probability distribution $P(\delta^2)$ of δ_{ab}^2 , which is obtained by averaging over the configurations a and b with the appropriate Boltzmann weights. In what follows we will use the mean

$$\langle \delta^2 \rangle = \int d\delta'^2 P(\delta'^2) \delta'^2, \quad (20)$$

which is small if the structural fluctuations are small, but tells nothing about the actual structure. In addition, we therefore measure the similarity to the desired structure r_0 . For this purpose we average δ_{ab}^2 over configuration a , keeping configuration b fixed and equal to r_0 . This average will be denoted by $\langle \delta_0^2 \rangle$.

As indicated above, when investigating thermodynamic properties of this model one finds a strong dependence upon the local interactions. This impact of local interactions is *not* a peculiar property for off-lattice models. Indeed, similar findings have been reported for the HP lattice model [20]. Furthermore, it has been claimed from 3D lattice studies that a two-letter code is not sufficient for native structure formation [3, 26], which is in contrast to the 3D off-lattice results reported in [11].

5.2 Design Results

Finding Suitable Structures

We have determined the global energy minima, or native structures, for a number of $N = 16$ sequences, and six of these structures are used as target structures in our design calculations. In addition, we consider six $N = 20$ target structures, which are native states of sequences studied in [11]. We restrict ourselves to these twelve examples because the verification of the design results, the computation of $\langle \delta_0^2 \rangle$, is time-consuming. This selection of structures studied represent no bias with respect to the performance of the design algorithm. As can be seen from Tables 6 and 7, some of the original sequences represent good folders (small $\langle \delta^2 \rangle$) whereas others do not (large $\langle \delta^2 \rangle$). An example of a target structure can be found in Fig. 11.

Designing the Sequences

As discussed above, in our off-lattice calculations, we use $P(\sigma)$ -based elimination, which, unlike $E(r, \sigma)$ -based elimination, can be used as it stands. All our design calculations are carried out at the temperature $T = 0.3$, whereas the highest folding temperatures measured in [11] are close to 0.2. This somewhat high design temperature was chosen in order to speed up the calculations. It is still low enough for design of stable sequences, as will become clear from the verification below. These verification calculations are performed at $T = 0.15$, using simulated tempering.

Our $P(\sigma)$ -based design calculations starts out from the set of all 2^N possible sequences. Each iterative step amounts to a relatively short multisequence simulation consisting of 500000 MC cycles for the N_r remaining sequences, followed by removal of those sequences for which the estimated $P(\sigma)$ fulfills Eq. (11) with $\Lambda = 1.5$. This is continued until a single sequence remains, which typically requires around 150 steps. The final sequence we take as the MS designed sequence. Each MC cycle consists of one attempt to update the conformation and one for the sequence. The conformation update is either a rotation of a single bond \hat{b}_i or a pivot move. The time consumption for the studied $N = 16$ and 20 chains ranges from three to six CPU hours.

The designed sequences are shown in Tables 6 and 7 for $N = 16$ and 20, respectively. Also shown are the results of “naive” energy minimization [2], which we implement with full exploration of binary patterns subject to a net hydrophobicity constraint. Ideally, one should perform this method by scanning through all possible N_H [Eq. (15)], which was done for $N \leq 18$ HP chains in Sec. 3.2. However, given that the verification is quite tedious, we have chosen to use a single N_H only, corresponding to the original sequence. In other words the $E(r_0, \sigma)$ -minimization method is given a slight advantage as compared to what would have been the case for a real-world application.

Verification

To assess the quality of the designed sequences, we measured the mean-square distances to their respective target structures, $\langle \delta_0^2 \rangle$, using simulated tempering. In Tables 6 and 7 we give both $\langle \delta_0^2 \rangle$ and $\langle \delta^2 \rangle$ [see Eq. (20)] at $T = 0.15$ for each of the sequences. From these tables a few features emerge:

- For target structures for which the original sequence is good (small $\langle \delta_0^2 \rangle$), the multisequence approach either returns the original sequence or finds an even better sequence.
- For target structures for which the original sequence is bad (high $\langle \delta_0^2 \rangle$), the multisequence approach often finds sequences with significantly lower $\langle \delta_0^2 \rangle$.
- With only one exception, structure 16-4, the results are better or much better for multisequence design than for the energy minimization method. For structure 16-4, the $\langle \delta_0^2 \rangle$ values are relatively high for both methods, as well as for the original sequence.

It should be stressed that in those instances where the multisequence approach fails to find a good sequence, the original sequence is bad, too. Hence, it is likely that these target structures do not represent designable structures.

	method	σ	$\langle \delta^2 \rangle_{T=0.15}$	$\langle \delta_0^2 \rangle_{T=0.15}$
16-1	target	1111100101101111	0.01 ± 0.0002	0.01 ± 0.002
	MS	1111100101111111	0.01 ± 0.0002	0.01 ± 0.002
	$E(r_0, \sigma)$	1111100101011111	0.02 ± 0.003	0.01 ± 0.007
16-2	target	1011001110011110	0.07 ± 0.003	0.04 ± 0.004
	MS	1011001110011110	0.03 ± 0.004	0.02 ± 0.007
	$E(r_0, \sigma)$	1111001010101110	0.38 ± 0.03	0.52 ± 0.02
16-3	target	1010101001101111	0.24 ± 0.05	0.13 ± 0.02
	MS	1111111101001111	0.01 ± 0.001	0.01 ± 0.006
	$E(r_0, \sigma)$	1010101101001111	0.08 ± 0.02	0.04 ± 0.02
16-4	target	1101101000010011	0.38 ± 0.02	0.25 ± 0.02
	MS	1111101111010011	0.12 ± 0.01	0.36 ± 0.01
	$E(r_0, \sigma)$	1010101000010111	0.28 ± 0.01	0.24 ± 0.02
16-5	target	1001110011111111	0.47 ± 0.02	0.33 ± 0.02
	MS	1001110010111111	0.12 ± 0.002	0.10 ± 0.01
	$E(r_0, \sigma)$	1011110010111111	0.11 ± 0.004	0.11 ± 0.01
16-6	target	1110010000000110	0.64 ± 0.007	0.57 ± 0.02
	MS	1101111101011111	0.30 ± 0.02	0.34 ± 0.02
	$E(r_0, \sigma)$	0101010000101010	0.28 ± 0.02	0.42 ± 0.01

Table 6: Design results for six $N = 16$ off-lattice target structures. For each structure three sequences are listed together with the corresponding $\langle \delta_0^2 \rangle$ (for completeness also $\langle \delta^2 \rangle$ are given): the sequence that was used to generate the target structure (“target”), and the two sequences obtained by multisequence design (**MS**) and $E(r_0, \sigma)$ -minimization, respectively.

While this very simple implementation of multisequence design has been tested with success, it should be kept in mind that there are a number of possible improvements. As already mentioned, it would, for example, in off-lattice problems be more natural to maximize the fuzzy version of the conditional probability in Eq. (4), rather than the one referring to a single structure r_0 used here.

6 Summary

A novel MC scheme for sequence optimization in coarse-grained protein models has been presented. With simultaneous moves in both sequence and conformation space according to a judiciously chosen joint distribution, an efficient way of maximizing the corresponding conditional probabilities emerges, in which two different prescriptions are given for removing sequences not suitable for the target structures. One of the prescriptions is a simple energy comparison that can be applied to lattice models, whereas the other one is based upon the marginal distribution $P(\sigma)$ and can be applied to both lattice and off-lattice models.

The potential memory problem of keeping track of removal of most of the 2^N sequences for large N is dealt with by an iterative method, capitalizing on the fact that the assignment of certain positions in the chain tend to get “frozen” to hydrophobic/polar residues.

The method is evaluated on a number of 2D lattice ($N = 16, 18, 32$ and 50) and 3D off-lattice

	method	σ	$\langle \delta^2 \rangle_{T=0.15}$	$\langle \delta_0^2 \rangle_{T=0.15}$
20-1	target	11110011110110111001	0.08 ± 0.01	0.04 ± 0.01
	MS	11110011110010111001	0.02 ± 0.001	0.01 ± 0.002
	$E(r_0, \sigma)$	1111001111110101001	0.27 ± 0.04	0.29 ± 0.01
20-2	target	11110110101100111011	0.27 ± 0.05	0.15 ± 0.01
	MS	11110100100100111111	0.02 ± 0.004	0.01 ± 0.003
	$E(r_0, \sigma)$	11110010101010111111	0.24 ± 0.05	0.93 ± 0.01
20-3	target	11100100101001010101	0.30 ± 0.04	0.38 ± 0.01
	MS	11111100101001010111	0.10 ± 0.02	0.12 ± 0.01
	$E(r_0, \sigma)$	10101000101001010111	0.59 ± 0.02	0.53 ± 0.01
20-4	target	01101111010110111110	0.24 ± 0.02	0.34 ± 0.01
	MS	01101010010111111110	0.05 ± 0.01	0.03 ± 0.01
	$E(r_0, \sigma)$	01101011010111111110	0.10 ± 0.01	0.05 ± 0.01
20-5	target	01111110111101101100	0.46 ± 0.04	0.29 ± 0.01
	MS	11111110100101111101	0.46 ± 0.04	0.43 ± 0.01
	$E(r_0, \sigma)$	01111110100101111101	0.65 ± 0.09	0.46 ± 0.01
20-6	target	01100111000101011010	0.73 ± 0.01	0.75 ± 0.01
	MS	11100111001101011111	0.64 ± 0.02	0.73 ± 0.01
	$E(r_0, \sigma)$	01111010100101001010	0.52 ± 0.08	0.91 ± 0.01

Table 7: Design results for six $N = 20$ off-lattice target structures. The corresponding sequences are those from Table 1 in [11] but here ordered according to decreasing $\langle \delta^2 \rangle$. Same notation as in Table 6.

($N = 16$ and 20) structures with the following results:

- For $N = 16$ and 18 lattice chains, where the results can be gauged against exact enumeration, the results come out extremely well both with respect to performance and efficiency. In this context we also compare with and discuss other non-exact approaches — $E(r_0, \sigma)$ -minimization and high- T expansion. With respect to the former, we give, in contrast to other comparisons in the literature, the approach a fair chance by scanning over all possible net hydrophobicities.
- For $N > 18$ lattice chains, finding suitable design structures and verifying good folding properties of the designed chains is not trivial. For $N = 32$ a suitable structure was designed "by hand", whereas for $N = 50$ a more systematic procedure was employed, where a variant of the multisequence approach was used to find any designable structure. For both $N = 32$ and $N = 50$ structures the results from the design procedure were verified to be correct.
- For $N = 16$ and $N = 20$ off-lattice chains, a set of structures representing both good and bad folders were used to test the design method. For good folding sequences, the design procedure either identifies the original sequence or finds a sequence with improved folding properties. In the case of bad folding sequences, the design procedure typically finds a sequence with improved folding properties.

In addition, having access to a good $N = 50$ HP sequence, we explored the behavior at the folding transition in terms of the distribution of the number of native contacts. In contrast to the general belief that 2D models do not exhibit cooperativity [14], and to previous results for shorter chains, we find an unambiguous sign of cooperativity for this chain length.

We also separately evaluate the efficiency of the multisequence approach as compared to standard MC for ordinary thermodynamic folding simulations. Such a test was carried out in [8] using carefully tuned parameters $g(\sigma)$. The results presented here show that it can be less expensive to fold 100–1000 chains simultaneously than a single one, even with a simple choice of $g(\sigma)$ [Eq. (9)].

Acknowledgement

This work was supported by the Swedish Foundation for Strategic Research, the Swedish Natural Research Council and the Swedish Council for High-Performance Computing.

Appendix: Lattice Monte Carlo Moves

Our simulations of the HP model have been performed using standard updates for self-avoiding walks. Three types of elementary moves were used: one-bead, two-bead and pivot [27]. Throughout the paper, a MC sweep refers to a combination of $N - 1$ one-bead steps, $N - 2$ two-bead steps and one pivot step. As is well-known, on its own such an algorithm becomes very slow in the compact low-temperature regime. In the dynamical-parameter approach, one tries to overcome this problem by promoting some parameter of the model to a dynamical variable. Hence, rather than inventing more clever elementary moves in conformation space, one adds updates of a new variable.

In our multisequence and simulated-tempering simulations each MC sweep in conformation space is followed by one attempt to update the sequence or temperature. The sequence and temperature updates are both ordinary Metropolis steps [28]. The CPU cost of these updates is negligible compared to that of the conformation update.

References

- [1] E.I. Shakhnovich and A.M. Gutin, “A New Approach to the Design of Stable Proteins”, *Protein Eng.* **6**, 793–800 (1993).
- [2] E.I. Shakhnovich and A.M. Gutin, “Engineering of Stable Fast-Folding Sequences of Model Proteins”, *Proc. Natl. Acad. Sci. USA* **90**, 7195–7199 (1993).
- [3] E.I. Shakhnovich, “Proteins with Selected Sequences Fold into Unique Native Conformation”, *Phys. Rev. Lett.* **72**, 3907–3910 (1994).
- [4] T. Kurosky and J.M. Deutsch, “Design of Copolymeric Materials”, *J. Phys. A* **27**, L387–L393 (1995).
- [5] J.M. Deutsch and T. Kurosky, “New Algorithm for Protein Design”, *Phys. Rev. Lett.* **76**, 323–326 (1996).
- [6] M.P. Morrissey and E.I. Shakhnovich, “Design of Proteins with Selected Thermal Properties”, *Fold. Des.* **1**, 391–405 (1996).
- [7] F. Seno, M. Vendruscolo, A. Maritan, and J.R. Banavar, “An Optimal Protein Design Procedure”, *Phys. Rev. Lett.* **77**, 1901–1904 (1996).
- [8] A. Irbäck and F. Potthast, “Studies of an Off-Lattice Model for Protein Folding: Sequence Dependence and Improved Sampling at Finite Temperature”, *J. Chem. Phys.* **103**, 10298–10305 (1995).
- [9] A. Irbäck, C. Peterson F. Potthast and E. Sandelin, “A Novel Monte Carlo Procedure for Protein Design”, LU TP 97-33, cond-mat/9711092 (to appear in *Phys. Rev. E*).
- [10] K.F. Lau and K.A. Dill, “A Lattice Statistical Model for the Conformational and Sequence Spaces of Proteins”, *Macromolecules* **22**, 3986–3997 (1989).
- [11] A. Irbäck, C. Peterson, F. Potthast and O. Sommelius, “Local Interactions and Protein Folding: A 3D Off-Lattice Approach”, *J. Chem. Phys.* **107**, 273–282 (1997).
- [12] A.P. Lyubartsev, A.A. Martsinovski, S.V. Shevkunov and P.N. Vorontsov-Velyaminov, “New Method to Monte Carlo Calculation of the Free Energy: Method of Expanded Ensembles”, *J. Chem. Phys.* **92**, 1776–1783 (1992).
- [13] E. Marinari and G. Parisi, “Simulated Tempering: A New Monte Carlo Scheme”, *Europhys. Lett.* **19**, 451–458 (1992).
- [14] E.I. Shakhnovich, “Theoretical Studies of Protein-Folding Thermodynamics and Kinetics”, *Curr. Opin. Struct. Biol.* **7**, 29–40 (1997).
- [15] A. Irbäck, C. Peterson and F. Potthast, “Identification of Amino Acid Sequences with Good Folding Properties”, *Phys. Rev. E* **55**, 860–867 (1997).
- [16] A. Irbäck, “Dynamical-Parameter Algorithms for Protein Folding”, LU TP 98-6, to appear in *Monte Carlo Approach to Biopolymers and Protein Folding*, eds. P. Grassberger, G. Barkema and W. Nadler (World Scientific).
- [17] K. Yue and K.A. Dill, “Forces of Tertiary Structural Organization in Globular Proteins”, *Proc. Natl. Acad. Sci. USA* **92**, 146–150 (1995).

- [18] H. Li, R. Helling, C. Tang and N. Wingreen, “Emergence of Preferred Structures in a Simple Model of Protein Folding”, *Science* **273**, 666–669 (1996).
- [19] H.S. Chan and K.A. Dill, “Transition States and Folding Dynamics of Proteins and Heteropolymers”, *J. Chem. Phys.* **100**, 9238–9257 (1994).
- [20] A.Irbäck and E. Sandelin, “Local Interactions and Protein Folding: A Model Study on the Square and Triangular Lattices”, *J. Phys. Chem.* **108**, 2245–2250 (1998).
- [21] V.I. Abkevich, A.M. Gutin and E.I. Shakhnovich, “Impact of Local and Non-local Interactions on Thermodynamics and Kinetics of Protein Folding”, *J. Mol. Biol.* **252**, 460–471 (1995).
- [22] K.A. Dill, S. Bromberg, K. Yue, K.M. Fiebig, P.D. Thomas and H.S. Chan, “Principles of Protein Folding — A Perspective from Simple Exact Models”, *Protein Sci.* **4**, 561–602 (1995).
- [23] T. Veitshans, D. Klimov and D. Thirumalai, “Protein Folding Kinetics: Timescales, Pathways, and Energy Landscapes in terms of Sequence-Dependent Properties”, *Fold. Des.* **2**, 1–22 (1997).
- [24] M. Sasai, “Conformation, Energy, and Folding Ability of Selected Amino Acid Sequences”, *Proc. Natl. Acad. Sci. USA* **92**, 8438–8442 (1995).
- [25] H. Nymeyer, A.E. Garcia and J.N. Onuchic, “Folding Funnels and Frustration in Off-Lattice Minimalist Protein Landscapes”, *Proc. Natl. Acad. Sci. USA* **95**, 5921–5928 (1998).
- [26] K. Yue, K.M. Fiebig, P.D. Thomas, H.S. Chan, E.I. Shakhnovich and K.A. Dill, “A Test of Lattice Protein Folding Algorithms”, *Proc. Natl. Acad. Sci. USA* **92**, 325–329 (1995).
- [27] See e.g. A.D. Sokal, “Monte Carlo Methods for the Self-Avoiding Walk”, in *Monte Carlo and Molecular Dynamics Simulations in Polymer Science*, ed. K. Binder (Oxford University Press, New York, 1995).
- [28] N. Metropolis, A.W. Rosenbluth, M.N. Rosenbluth, A.H. Teller and E. Teller, “Equation of State Calculations by Fast Computing Machines”, *J. Chem. Phys.* **21**, 1087–1092 (1953).